



## Discovery of novel oxazolidinedione derivatives as potent and selective mineralocorticoid receptor antagonists

Christine Yang<sup>a,\*</sup>, Hong C. Shen<sup>a,\*</sup>, Zhicai Wu<sup>a</sup>, Hong D. Chu<sup>a</sup>, Jason M. Cox<sup>a</sup>, Jaume Balsells<sup>b</sup>, Alejandro Crespo<sup>c</sup>, Patricia Brown<sup>e</sup>, Beata Zamlyny<sup>e</sup>, Judyann Wiltsie<sup>d</sup>, Joseph Clemas<sup>d</sup>, Jack Gibson<sup>d</sup>, Lisa Contino<sup>d</sup>, JeanMarie Lisnock<sup>d</sup>, Gaochao Zhou<sup>d</sup>, Margarita Garcia-Calvo<sup>d</sup>, Tom Bateman<sup>f</sup>, Ling Xu<sup>f</sup>, Xinchun Tong<sup>f</sup>, Martin Crook<sup>e</sup>, Peter Sinclair<sup>a</sup>

<sup>a</sup> Department of Discovery Chemistry, Merck Research Laboratories, PO Box 2000, Rahway, NJ 07065-0900, USA

<sup>b</sup> Department of Process Chemistry, Merck Research Laboratories, PO Box 2000, Rahway, NJ 07065-0900, USA

<sup>c</sup> Department of Chemistry Modeling & Information, Merck Research Laboratories, PO Box 2000, Rahway, NJ 07065-0900, USA

<sup>d</sup> Department of In Vitro Pharmacology, Merck Research Laboratories, PO Box 2000, Rahway, NJ 07065-0900, USA

<sup>e</sup> Department of Cardiovascular Diseases, Merck Research Laboratories, PO Box 2000, Rahway, NJ 07065-0900, USA

<sup>f</sup> Department of Drug Metabolism, Merck Research Laboratories, PO Box 2000, Rahway, NJ 07065-0900, USA

### ARTICLE INFO

#### Article history:

Received 21 March 2013

Revised 20 May 2013

Accepted 21 May 2013

Available online 4 June 2013

#### Keywords:

Mineralocorticoid receptor antagonist

Hypertension

### ABSTRACT

Novel oxazolidinedione analogs were discovered as potent and selective mineralocorticoid receptor (MR) antagonists. Structure–activity relationship (SAR) studies were focused on improving the potency and microsomal stability. Selected compounds demonstrated excellent MR activity, reasonable nuclear hormone receptor selectivity, and acceptable rat pharmacokinetics.

© 2013 Elsevier Ltd. All rights reserved.

The mineralocorticoid receptor (MR) is a nuclear hormone receptor that regulates the expression of multiple genes involved in cardiovascular disease and electrolyte homeostasis. MR is activated by aldosterone, which increases blood pressure through its effects on natriuresis, with potential additional effects on the brain, heart and vasculature.<sup>1</sup> In visceral tissues, such as the kidney and the gut, MR regulates sodium retention, potassium excretion and water balance in response to aldosterone. Resistant hypertensive patients frequently suffer from increased aldosterone levels, often termed as ‘aldosterone breakthrough’, as a result of increases in serum potassium or residual subtype I receptor activity of angiotensin II (AT1R).<sup>2</sup> Hyperaldosteronism and aldosterone breakthrough typically cause elevated blood pressure and congestive heart failure (CHF), as well as enhanced MR activity. Hence, direct antagonism of MR has a strong biological rationale for treating hypertension and CHF.

Other receptors in the same receptor subclass are androgen receptor (AR), glucocorticoid receptor (GR), estrogen receptor (ER), and the progesterone receptor (PR). It should be noted that both cortisol and corticosterone bind MR, and aldosterone is generally considered as the major endogenous ligand for MR with high

affinity.<sup>3</sup> Due to the distinct functions of each nuclear hormone receptor, it is imperative to develop selective MR antagonists to minimize potential side effects as a result of interaction with other nuclear hormone receptors.

Despite significant therapeutic advances in the treatment of hypertension and heart failure, the current standard of care is sub-optimal and there is a clear unmet medical need for additional pharmacological interventions. Eplerenone and spironolactone are two MR antagonists that are efficacious in treating cardiovascular disease, particularly hypertension and heart failure.<sup>4</sup> Moreover, multiple studies have shown that treatment with spironolactone or eplerenone significantly lower systolic blood pressure in hypertensive patients.<sup>5</sup> In spite of their therapeutic utility, there remain issues to overcome for both eplerenone and spironolactone. For example, spironolactone elicits unwanted side effects such as gynecomastia and menstrual irregularities due to its AR and PR activity.<sup>6</sup> Conversely, eplerenone is more selective against other nuclear hormone receptors, but it lacks good MR potency relative to spironolactone and requires b.i.d. dosing.<sup>7</sup> As such, we have embarked on a discovery program to identify efficacious and safe MR antagonists that possess the efficacy of spironolactone and selectivity of eplerenone. Herein we report preliminary results on the discovery of oxazolidinedione derivatives as a class of novel, non-steroidal, and potent MR antagonists.<sup>8</sup>

\* Corresponding authors. Tel.: +1 908 740 6593.

E-mail address: [christine\\_yang@merck.com](mailto:christine_yang@merck.com) (C. Yang).

An in-house high-throughput screening identified compound **1a** with modest MR activity in the human MR NH Pro assay ( $IC_{50} = 6 \mu M$ ). This assay is a commercially available PathHunter™ protein–protein interaction assay that measures the ability of compounds to antagonize full-length human MR binding to a coactivator peptide.<sup>9</sup> In this assay, the average  $IC_{50}$  for spironolactone and eplerenone is 11 nM and 244 nM, respectively. Hit **1a** possesses at least four distinct subgroups as colored in Figure 1. The optimization strategy is to establish SAR with each of the four subgroups, namely,  $R^1$ – $R^3$  and the oxazolinedione core, as summarized in Tables 1–4.

Prior to the optimization of  $R^1$  region in **1a** (Table 1), the influence of the absolute configuration of **1a** on MR antagonism was found to be critical with the enantiomer of **1a** being essentially inactive ( $IC_{50} > 40 \mu M$ ). In addition, 3-OMe substitution of the benzyl group (**1b**) improved the MR activity by sixfold compared to **1a**. The next discovery was that the methyl group present in the  $R^3$  region markedly enhanced the activity against MR (**1c** vs **1b** and **1g** vs **1f**). With this embedded methyl group in the  $R^3$  region, various substitution of the benzyl group were explored (**1h–1o** are shown as a subset), however, none exhibited superior activity to **1g**. On the other hand, the presence of the methyl group in the  $R^1$  region of **1j** and **1k** did not present advantages over compound **1i** in terms of activity. Fused bicyclic aryl or heteroaryl methyl amine-derived amides, in general, led to reduced MR activity (**1p**, **1jj**, **1kk** and **1ll**), except in the case of **1mm**. The incorporation of monocyclic heteroaryls one or two carbons away from the amide group, as shown by **1dd–1ii** and **1nn–1qq**, respectively, resulted in poor MR activity. The size variation of cycloalkyl groups adjacent to amide gave MR activities within a few-fold of fluctuation (**1x–1z**). The addition of a terminal phenyl group to cyclobutyl or cyclopropyl improved potency as shown by **1aa–1cc**. Lastly, aniline analogs (**1q–1w**) provided modest to good potency.

Table 2 summarizes the efforts to optimize the  $R^2$  region. The removal of the benzyl group in this region resulted in a complete loss of activity against MR (**2a** vs **1a**). The binding pocket of  $R^2$  appeared to be non-polar as heteroaryl analogs (**2b–2d**, **2l** and **2m**) led to significant loss of activity. In addition, the size of the binding pocket may be small; larger fused bicyclic groups (**2k**, **2l** and **2m**), or chlorine substitution (**2h–2j**) were associated with at least eightfold decrease in MR potency. Lastly, the only acceptable substitution on the benzyl group appeared to be fluorine (**2e–2g**) despite the loss of four to sixfold potency.

The SAR for the  $R^3$  area is depicted in Table 3. First, the phenyl group in the  $R^3$  region of analog **1g** contributed significantly to its activity against MR. The absence of this group caused a ~10-fold loss of activity (**3a** vs **1g**). Second, the chirality of the stereogenic center in this region is important for biological activity against MR. For example, diastereomer **3b** is 10-fold less active than **1g**. Fluoro- and chloro-substitution (**3c** and **3d**, respectively) maintained excellent activity. Cyclohexyl analog **3e** was the most potent MR antagonist that we found for this series with an  $IC_{50}$  of 14 nM. By introducing a ring fused to the phenyl group, indanyl and tetrahydronaphthyl derivatives rendered  $IC_{50}$  of 33 and 170 nM, respectively. Interestingly, **3h**, a one-carbon homolog of **1g**, was much

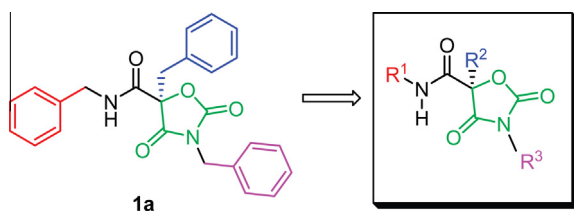


Figure 1. Pharmacophore of the oxazolinedione series.

Table 1  
In vitro SAR of  $R^1$  moiety in the human MR NH Pro assay<sup>a</sup>

| Compds   | $IC_{50}$ ( $\mu M$ ) | Compds   | $IC_{50}$ ( $\mu M$ ) |
|--|-----------------------|--|-----------------------|
| $R^1 = \text{Bn}, R = \text{H}$ ( <b>1a</b> )                          | 6.0                   | $R^1 = 3\text{-F-phenyl}$<br>$R = \text{Me}$ ( <b>1v</b> )       | 0.30                  |
| Enantiomer of <b>1a</b>  | >40                   | $R^1 = 4\text{-CN-phenyl}$<br>$R = \text{Me}$ ( <b>1w</b> )      | 0.10                  |
| $R^1 = 3\text{-OMe-benzyl}$<br>$R = \text{H}$ ( <b>1b</b> )            | 1.0                   | $R^1 = \text{Cyclohexyl}, R = \text{Me}$ ( <b>1x</b> )           | 4.0                   |
| $R^1 = 3\text{-OMe-benzyl}$<br>$R = \text{Me}$ ( <b>1c</b> )           | 0.3                   | $R^1 = \text{Cyclobutyl}, R = \text{Me}$ ( <b>1y</b> )           | 1.2                   |
| $R^1 = 4\text{-OMe-benzyl}$<br>$R = \text{Me}$ ( <b>1d</b> )           | 1.0                   | $R^1 = \text{Cyclopropyl}, R = \text{Me}$ ( <b>1z</b> )          | 2.0                   |
| $R^1 = 2\text{-OMe-benzyl}$<br>$R = \text{Me}$ ( <b>1e</b> )           | 0.5                   | $R^1 = \text{Cyclobutyl}, R = \text{Me}$ ( <b>1aa</b> )          | 0.65                  |
| $R^1 = 3,5\text{-diOMe-benzyl}$<br>$R = \text{H}$ ( <b>1f</b> )        | 3.0                   | $R^1 = \text{Cyclopropyl}, R = \text{Me}$ ( <b>1bb</b> )         | 0.19                  |
| $R^1 = 3,5\text{-diOMe-benzyl}$<br>$R = \text{Me}$ ( <b>1g</b> )       | 0.054                 | $R^1 = \text{Cyclopropyl}, R = \text{Me}$ ( <b>1cc</b> )         | 0.25                  |
| $R^1 = 4\text{-Cl-benzyl}$<br>$R = \text{Me}$ ( <b>1h</b> )            | 0.20                  | $R^1 = \text{Imidazol-2-ylmethyl}, R = \text{Me}$ ( <b>1dd</b> ) | 3.0                   |
| $R^1 = 3\text{-Cl-benzyl}$<br>$R = \text{Me}$ ( <b>1i</b> )            | 0.28                  | $R^1 = \text{Imidazol-4-ylmethyl}, R = \text{Me}$ ( <b>1ee</b> ) | >10                   |
| $R^1 = \text{2-chlorophenyl}, R = \text{Me}$ ( <b>1j</b> )             | 0.40                  | $R^1 = \text{Imidazol-5-ylmethyl}, R = \text{Me}$ ( <b>1ff</b> ) | >40                   |
| $R^1 = \text{3-chlorophenyl}, R = \text{Me}$ ( <b>1k</b> )             | 2.6                   | $R^1 = \text{Imidazol-2-ylmethyl}, R = \text{Me}$ ( <b>1gg</b> ) | 13                    |
| $R^1 = 4\text{-CF}_3\text{-benzyl}$<br>$R = \text{Me}$ ( <b>1l</b> )   | 0.57                  | $R^1 = \text{Imidazol-4-ylmethyl}, R = \text{Me}$ ( <b>1hh</b> ) | 16                    |
| $R^1 = 3\text{-CF}_3\text{-benzyl}$<br>$R = \text{Me}$ ( <b>1m</b> )   | 0.50                  | $R^1 = \text{Imidazol-5-ylmethyl}, R = \text{H}$ ( <b>1ii</b> )  | >40                   |
| $R^1 = 4\text{-SO}_2\text{Me-benzyl}$<br>$R = \text{Me}$ ( <b>1n</b> ) | >10                   | $R^1 = \text{Indol-3-ylmethyl}, R = \text{Me}$ ( <b>1jj</b> )    | 2.5                   |
| $R^1 = 3\text{-SO}_2\text{Me-benzyl}$<br>$R = \text{Me}$ ( <b>1o</b> ) | 3.0                   | $R^1 = \text{Indol-2-ylmethyl}, R = \text{Me}$ ( <b>1kk</b> )    | 1.5                   |
| $R^1 = 2\text{-Naphthyl}$<br>$R = \text{Me}$ ( <b>1p</b> )             | 0.6                   | $R^1 = \text{Indol-1-ylmethyl}, R = \text{Me}$ ( <b>1ll</b> )    | 3.0                   |
| $R^1 = \text{2-fluorophenyl}, R = \text{Me}$ ( <b>1q</b> )             | 0.27                  | $R^1 = \text{Indol-3-ylmethyl}, R = \text{Me}$ ( <b>1mm</b> )    | 0.3                   |
| $R^1 = 4\text{-Cl-phenyl}$ ( <b>1r</b> )                               | 0.18                  | $R^1 = \text{Imidazol-2-ylmethyl}, R = \text{Me}$ ( <b>1nn</b> ) | 4.0                   |
| $R^1 = 3\text{-Cl-phenyl}$<br>$R = \text{Me}$ ( <b>1s</b> )            | 2.0                   | $R^1 = \text{Imidazol-4-ylmethyl}, R = \text{Me}$ ( <b>1oo</b> ) | 15                    |
| $R^1 = 2\text{-Cl-phenyl}$<br>$R = \text{Me}$ ( <b>1t</b> )            | 1.0                   | $R^1 = \text{Imidazol-5-ylmethyl}, R = \text{Me}$ ( <b>1pp</b> ) | >40                   |
| $R^1 = 4\text{-F-phenyl}$<br>$R = \text{Me}$ ( <b>1u</b> )             | 0.10                  | $R^1 = \text{Imidazol-2-ylmethyl}, R = \text{Me}$ ( <b>1qq</b> ) | >40                   |

<sup>a</sup> Values are based on the average of two experiments, each in 10-point titrations.

less active than **1g**. A heterocyclic analog (**3i**), or pyridyl replacement of the phenyl of **1g** led to more than 50-fold loss of MR potency. The combination of fluoro- and chloro-substituted phenyl groups resulted in **3j**, which displayed modest activity against MR.

The oxazolinedione core was also a subject of modification (Table 4). Almost all core modifications, as shown by analogs

**Table 2**  
In vitro SAR of R<sup>2</sup> moiety in the human MR NH Pro assay<sup>a</sup>

| Comps                                   | IC <sub>50</sub> (μM) | Comps                                   | IC <sub>50</sub> (μM) |
|---|-----------------------|---|-----------------------|
|   |                       |   |                       |
| R <sup>2</sup> = H, R = H ( <b>2a</b> ) | >40                   | R <sup>2</sup> = , R = Me ( <b>2g</b> ) | 0.30                  |
| R <sup>2</sup> = , R = H ( <b>2b</b> )  | >40                   | R <sup>2</sup> = , R = Me ( <b>2h</b> ) | >40                   |
| R <sup>2</sup> = , R = H ( <b>2c</b> )  | 30                    | R <sup>2</sup> = , R = Me ( <b>2i</b> ) | 0.75                  |
| R <sup>2</sup> = , R = Me ( <b>2d</b> ) | 3.0                   | R <sup>2</sup> = , R = Me ( <b>2j</b> ) | 0.45                  |
| R <sup>2</sup> = , R = Me ( <b>1g</b> ) | 0.054                 | R <sup>2</sup> = , R = Me ( <b>2k</b> ) | >40                   |
| R <sup>2</sup> = , R = Me ( <b>2e</b> ) | 0.20                  | R <sup>2</sup> = , R = Me ( <b>2l</b> ) | >40                   |
| R <sup>2</sup> = , R = Me ( <b>2f</b> ) | 0.28                  | R <sup>2</sup> = , R = Me ( <b>2m</b> ) | >40                   |

<sup>a</sup> Values are based on the average of two experiments, each in 10-point titrations.

**Table 3**  
In vitro SAR of R<sup>3</sup> moiety in the human MR NH Pro assay<sup>a</sup>

| Comps             | IC <sub>50</sub> (μM) | Comps           | IC <sub>50</sub> (μM) |
|-------------------|-----------------------|-----------------|-----------------------|
|                   |                       |                 |                       |
| iPr ( <b>3a</b> ) | 0.50                  | , ( <b>3f</b> ) | 0.033                 |
| , ( <b>1g</b> )   | 0.054                 | , ( <b>3g</b> ) | 0.17                  |
| , ( <b>3b</b> )   | 0.50                  | , ( <b>3h</b> ) | 0.40                  |
| , ( <b>3c</b> )   | 0.037                 | , ( <b>3i</b> ) | 2.9                   |
| , ( <b>3d</b> )   | 0.055                 | , ( <b>3j</b> ) | 0.18                  |
| , ( <b>3e</b> )   | 0.014                 |                 |                       |

<sup>a</sup> Values are based on the average of two experiments, each in 10-point titrations.

**Table 4**  
In vitro SAR of the oxazolidinedione core in the human MR NH Pro assay<sup>a</sup>

| Comps       | IC <sub>50</sub> (μM) | Comps                                   | IC <sub>50</sub> (μM) |
|-------------|-----------------------|---|-----------------------|
|             |                       |   |                       |
| <b>(4a)</b> | >40                   | <b>(4e)</b>                             | >40                   |
|             |                       |   |                       |
| <b>(4b)</b> | >40                   | <b>(4f)</b>                             | >10                   |
|             |                       |   |                       |
| <b>(4c)</b> | >40                   | <b>(4g)</b>                             | >40                   |
|             |                       |   |                       |
| <b>(4d)</b> | >40                   | <b>(4h) X = O</b><br><b>(4i) X = NH</b> | 0.34<br>0.99          |

<sup>a</sup> Values are based on the average of two experiments, each in 10-point titrations.

**4a–4g**, resulted in essentially a complete loss of activity against MR, except for tertiary amide **4i**, which only suffered a threefold loss in potency compared to **4h**.

Molecular modeling was employed to understand the potential binding mode of the oxazolidinedione derivatives. **Figure 2** shows the predicted binding orientation of compound **1g** obtained by molecular docking using the 1.95 Å MR X-ray structure 2A31.<sup>10</sup> The R<sup>1</sup> substituent is located in the A-ring pocket, making an edge-to-face π–π interaction with F829. The orientation and size of R<sup>1</sup> substituent are both critical for activity: from the electrophilic potentials (blue iso-surface mesh in **Fig. 2**), positions 3 and 5 of the benzyl ring at R<sup>1</sup> are favored. Thus, the OMe groups in **1g** interact with R817 (resembling the sterol A-ring 3-keto group) and non-conserved S810, resulting in the most potent substitutions in R<sup>1</sup>. Hydrophobic substitutions in the R<sup>1</sup> benzyl ring may also be tolerated (**1h**, **1i** and **1l**), due to the hydrophobic nature of the A-ring region. Incorporation of heteroaryl groups (**1dd–1ii**) show reduced activity since the acceptor group is not placed correctly to interact with R817. Moreover, increasing the R<sup>1</sup> substituent size (**1jj–1qq**) will reduce activity due to steric hindrance. Finally, replacing the R<sup>1</sup> benzyl group with a phenyl group, will favor substitutions at the 4 position with either halogen atoms or a cyano group (**1u** or **1w**).

Not only is the presence of a benzyl group in the R<sup>2</sup> region crucial for activity, but also its absolute configuration. The benzyl group is placed in the sterol D-ring pocket and interacts with L848, L938 and F941. The nature of the D-ring region is mostly hydrophobic (green iso-surface mesh in **Fig. 2**), hence polar analogs are less potent. Moreover, the benzyl ring completely fills the D-ring pocket, making the small fluorine analog the only acceptable substitution.

The methyl group in the R<sup>3</sup> position of **1g** contributes to MR activity by forcing the molecule to adopt the preferred bound orientation: the benzyl ring in R<sup>3</sup> is placed parallel to the benzyl ring in R<sup>2</sup>, making strong π–π interactions. The other stereoisomer in R<sup>3</sup>

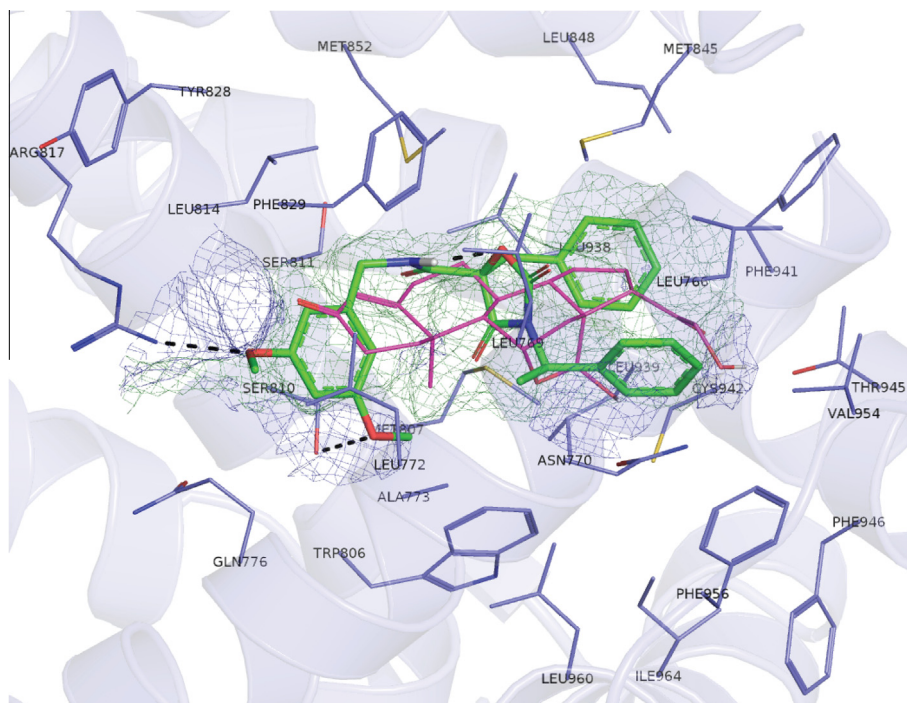


**Figure 2.** Suggested binding mode of **1g** within MR pocket: representative docking pose of compound **1g** (green sticks) in 2A31 MR ligand binding crystal structure. Side chains of residues located within 5 Å of **1g** are represented as blue lines. The electrophilic (blue) and hydrophobic (green) potentials within the binding pocket are shown as mesh representations. The dashed black lines illustrate atom pairs within hydrogen bond distance. Aldosterone crystal structure conformation is depicted as magenta lines for comparison.

**Table 5**  
Nuclear hormone receptor selectivity of **3f** and **3j**

| Compd          | MR  | GR   | GR  | AR   | AR  | ER $\alpha$  | ER $\alpha$   | ER $\beta$   | ER $\beta$  | PR $\beta$   | PR $\beta$  |
|----------------|---|--|---|--|---|--|---|--|---|--|---|
|                | NH_PRO<br>IC <sub>50</sub> ( $\mu$ M)<br>antagonist<br>mode | NH_PRO<br>EC <sub>50</sub> ( $\mu$ M)<br>agonist<br>mode | NH_PRO<br>IC <sub>50</sub> ( $\mu$ M)<br>antagonist<br>mode | NH_PRO<br>EC <sub>50</sub> ( $\mu$ M)<br>agonist<br>mode | NH_PRO<br>IC <sub>50</sub> ( $\mu$ M)<br>antagonist<br>mode | NH_PRO<br>EC <sub>50</sub> ( $\mu$ M)<br>agonist<br>mode | NH_PRO<br>IC <sub>50</sub> ( $\mu$ M)<br>antagonist<br>mode | NH_PRO<br>EC <sub>50</sub> ( $\mu$ M)<br>agonist<br>mode | NH_PRO<br>IC <sub>50</sub> ( $\mu$ M)<br>antagonist<br>mode | NH_PRO<br>EC <sub>50</sub> ( $\mu$ M)<br>agonist<br>mode | NH_PRO<br>IC <sub>50</sub> ( $\mu$ M)<br>antagonist<br>mode |
| Spironolactone | 0.011   | >20  | 4.1   | >20  | 0.67  | >20  | >20   | 3.3  | >20   | >20  | 4.0   |
| Eplerenone     | 0.24  | >20  | 18  | >20  | >20   | >20  | >20   | >20  | >20   | >20  | >20   |
| <b>3f</b>      | 0.033   | >20  | >20   | >20  | 12  | >20  | 17  | >20  | 15  | >20  | 8.1   |
| <b>3j</b>      | 0.18  | >20  | 11  | >20  | >20   | >20  | 7.3   | >20  | 15  | >20  | 3.6   |

**Table 6**  
Rat PK profiles of representative compounds<sup>a</sup>

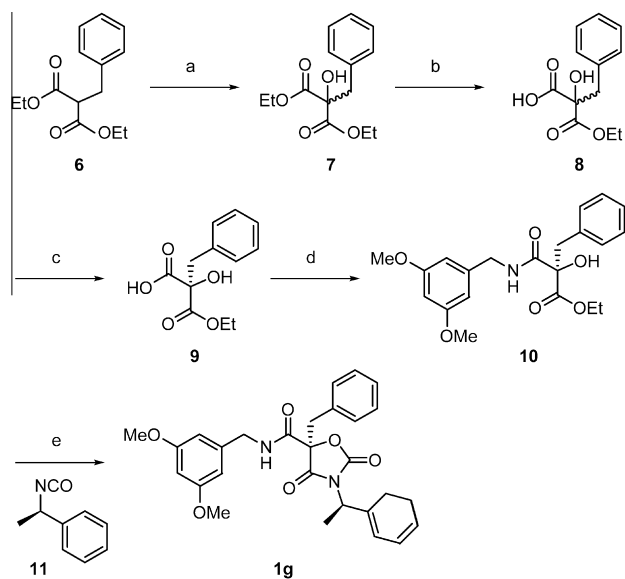
| Compd     | F (%) | Cl (mL/min/kg) | Vd <sub>ss</sub> (L/kg) | C <sub>max</sub> ( $\mu$ M) | T <sub>1/2</sub> (h) | AUCN iv, po ( $\mu$ M h kg/mg) |
|-----------|-------|----------------|-------------------------|-----------------------------|----------------------|--------------------------------|
| <b>1g</b> | 7     | 46             | 2.8                     | 0.06                        | 1.2                  | 0.75, 0.05                     |
| <b>3f</b> | 28    | 35             | 4.7                     | 0.098                       | 2.5                  | 0.89, 0.24                     |
| <b>3j</b> | 63    | 66             | 7.9                     | 0.12                        | 2.3                  | 0.46, 0.24                     |

<sup>a</sup> Formulation: 1 mg/mL PEG 200: water (70:30). iv Dose: 1 mg/kg ( $n = 2$ ). po Dose: 1 mg/kg ( $n = 3$ ). Blood concentrations were determined by LC/MS/MS following protein precipitation with acetonitrile.

will not promote this bound conformation, hence reducing its activity against MR. The methyl group also interacts with MR by protecting the backbone hydrogen-bond between hydrophobic residues L769 and A773 located in helix 3. From the iso-surface mesh in Figure 2, position 4 of the benzyl ring is ideal for substitution, as reported for compounds **3c** and **3d**. Compounds **3e–3g** will bind similarly with their R<sup>3</sup> groups interacting with hydrophobic residues located in helix 3 (L766, N770, L769 and A773), the loop preceding helix 12 (V954 and F956) and helix 12 (L960). However, the ethyl group in compound **3h** will clash with helix 3. Interestingly, the location of the benzyl ring in R<sup>3</sup> coincides with the region where aldosterone's C-18 OH and C-21 OH groups are bound. This orientation will prevent the formation of the canonical hydrogen

bond network (between the ligand, N770 in helix 3 and T945 in helix 10) required for receptor activation,<sup>11</sup> making the R<sup>3</sup> region an important feature contributing to the antagonism of MR.

The oxazolidinedione core binds in the hydrophobic C-ring region of the pocket and it is oriented perpendicular to both the steroid plane and R<sup>2</sup>/R<sup>3</sup> benzyl rings (Fig. 2). Although it does not make any direct interaction with polar atoms of MR, the oxazolidinedione core is essential for activity since it constrains the molecule to adopt the desired bound conformation by placing the R<sup>1–3</sup> groups in the correct pocket regions. The O-atom also makes an important intramolecular hydrogen bond with the amide group of R<sup>1</sup> (Fig. 2). Removal of the O-atom or the carbonyl groups will increase conformational flexibility of the molecule and disrupt the



**Scheme 1.** Reagents and conditions: (a) CsF, DMF, 40 °C to rt, 3 days, 71%; (b) KOH, EtOH, 46%, rt, overnight; (c) chiral SFC (OJ-H, 4.6 × 100 mm, 5% MeOH/0.1% TFA/CO<sub>2</sub>, 2.5 mL/min, 100 bar); (d) HATU, *i*Pr<sub>2</sub>NEt, 3,5-dimethoxybenzylamine, DMF, 2 h, 72%; (e) **11**, NaOH, THF, rt, overnight, 57%.

placement of the R<sup>2</sup>/R<sup>3</sup> benzyl rings in the ligand binding pocket, reducing its activity. Furthermore, the reported binding mode has strain energy of 2 kcal/mol, which is thermally accessible at room temperature.

The selectivity profiles of representative analogs **3f** and **3j** against several nuclear hormone receptors, including AR, GR, ER $\alpha$ , ER $\beta$ , and PR $\beta$ , are shown in Table 5. Compounds **3f** and **3j** demonstrated acceptable selectivity, in particular, superior selectivity in the AR antagonist mode assay with respect to spironolactone.

The rat pharmacokinetic (PK) profiles of compounds **1g**, **3f** and **3j** are shown in Table 6. All compounds exhibited modest to high clearance and acceptable IV exposure, with **1g** showing poor oral bioavailability. Interestingly, the structurally closely related and more conformationally constrained analog **3g**, improved the oral bioavailability to 28%. The best oral bioavailability was observed with **3j** (63%). The preliminary PK studies demonstrated that the oxazolidinedione represented a promising lead series.

A representative synthesis of oxazolidinedione analogs is illustrated in Scheme 1.<sup>12</sup> The  $\alpha$ -hydroxylation of malonate **6** occurred by applying vigorous air bubbling over 3 days, to afford desired hydroxylated intermediate **7**, which then underwent a monohydrolysis to yield monocarboxylic acid **8**. Chiral super critical fluid chromatography (SFC) separation provided the chiral acid **9**, which subsequently coupled with 3,5-dimethoxybenzylamine to generate amide **10**. The final oxazolidinedione formation was accomplished by using isocyanate **11** in the presence of solid NaOH in THF. It should be noted that the oxazolidinedione is particularly unstable under basic aqueous conditions.

In conclusion, we have identified novel oxazolidinedione amides as potent antagonists for MR. Systematic SAR studies led to several compounds with excellent selectivity over other nuclear hormone receptors, and representative compounds also displayed reasonable PK profiles in rats. Further investigations of the series will be reported in due course.

## References and notes

- Fardella, C.; Miller, W. *Annu. Rev. Nutr.* **1996**, *16*, 443.
- McKelvie, R. S.; Yusuf, S.; Pericak, D.; Avezum, A.; Burns, R. J.; Probstfield, J.; Tsuyuki, R. T.; White, M.; Rouleau, J.; Latini, R.; Maggioni, A.; Young, J.; Pogue, J. *Circulation* **1999**, *100*, 1056.

- Funder, J. W. *Annu. Rev. Med.* **1997**, *48*, 231.
- (a) The RALES Investigators *N. Eng. J. Med.* **1999**, *341*, 709; (b) Zannad, F.; McMurray, J. J. V.; Krum, H.; van Veldhuisen, D. J.; Swedberg, K.; Shi, H.; Vincent, J.; Pocock, S. J.; Pitt, B. *N. Eng. J. Med.* **2003**, *348*, 1309; (c) Funder, J. W. *Hypertens. Res.* **2010**, *33*, 539.
- (a) Calhoun, D. A.; White, W. B. *J. Am. Soc. Hypertens.* **2008**, *2*, 462; (b) The RALES Investigators *Am. J. Cardiol.* **1996**, *78*, 902; (c) Bomback, A. S.; Muskala, P.; Bald, E.; Chwatko, G.; Nowicki, M. *Clin. Nephrol.* **2009**, *72*, 449; (d) Williams, J. S. *Nat. Rev. Endocrinol.* **2010**, *6*, 248; (e) Nishizaka, M. K.; Calhoun, D. A. *Curr. Hypertens. Rep.* **2005**, *7*, 343; (f) Gaddam, K.; Corros, C.; Pimenta, E.; Ahmed, M.; Denney, T.; Aban, I.; Inusah, S.; Gupta, H.; Lloyd, S. G.; Oparil, S.; Husain, A.; Dell'Italia, L. J.; Calhoun, D. A. *Hypertension* **2010**, *55*, 1137; (g) Zannad, F.; McMurray, J. J.; Drexler, H.; Drum, H.; van Veldhuisen, D. J.; Swedberg, K.; Shi, H.; Vincent, J.; Pitt, B. *Eur. J. Heart Fail.* **2010**, *12*, 617.
- De Gasparo, M.; Whitebread, S. E.; Preiswerk, G.; Jeunemaitre, X.; Corvol, P.; Menard, J. *Steroid Biochem.* **1989**, *32*, 223.
- De Gasparo, M.; Joss, U.; Ramjoe, H.; Whitebread, S.; Haenni, H.; Schenkel, L.; Kraehenbuehl, C.; Biollas, M.; Grob, J.; Schmidlin, J.; Wieland, P.; Wehrli, H. U. *J. Pharmacol. Exp. Ther.* **1987**, *240*, 650.
- For other non-steroidal MR antagonists, see review: Meyers, M. J.; Hu, X. *Expert Opin. Ther. Pat.* **2007**, *17*, 17.
- <http://www.discoverx.com/nhrs/prod-nhrs.php>.
- Molecular modeling was performed starting from the 1.95 Å MR structure with bound corticosterone (PDB code 2A31; Li, Y.; Suino, K.; Daugherty, J.; Xu, H. E. *Mol. Cell.* **2005**, *19*, 367). The structure was prepared by removal of waters, addition of hydrogens, and restrained energy minimization using MacroModel (MacroModel 9.8.107, Schrödinger LLC, New York, NY). Electrostatic and hydrophobic potentials were generated with Maestro (Maestro 9.1.107, Schrödinger LLC, New York, NY) in a 6 Å grid centered on the crystallographic ligand. Molecular docking was performed by employing our in-house docking routine FLOG (Miller, M. D.; Kearsley, S. K.; Underwood, D. J.; Sheridan, R. P. *J. Comput. Aided Mol. Des.* **1994**, *8*, 153), which ranks pre-calculated conformations of the target molecules in a 6 Å grid centered on the crystallographic ligand. Conformations were generated using our in-house metric matrix distance geometry algorithm JG (Kearsley, S. K. Merck & Co., Inc., unpublished). The conformations were subjected to energy minimization with MacroModel using the MMFFs force field (Halgren, T. A. *J. Comput. Chem.* **1999**, *20*, 720). The representative docking pose reported in Figure 2 was selected by visual inspection using SAR and was subjected to restrained energy minimization (using MacroModel) to produce the model shown. Figure 2 was generated using Pymol (The Pymol Molecular Graphics System, version 1.4, Schrödinger LLC, New York, NY).
- Bledsoe, R. K.; Madauss, K. P.; Holt, J. A.; Apolito, C. J.; Lambert, M. H.; Pearce, K. H.; Stanley, T. B.; Stewart, E. L.; Trump, R. P.; Willson, T. M.; Williams, S. P. *J. Biol. Chem.* **2005**, *280*, 31283.
- The mixture of diethyl  $\alpha$ -benzylmalonate (41 g, 164 mmol) and CsF (49.8 g) in 90 mL of DMF was heated at 40 °C with vigorous air bubbling for 3 days. The resulting mixture was diluted with ethyl acetate (800 mL) and washed with water (1 L × 3). The organic layer was concentrated and then purified by biotage (5–20% ethyl acetate in hexanes) to give the diethyl  $\alpha$ -benzyl  $\alpha$ -hydroxy malonate (31 g, 117 mmol, 71%) as a colorless oil. <sup>1</sup>H NMR (300 MHz, CDCl<sub>3</sub>)  $\delta$ : 7.22–7.26 (m, 5H), 4.23 (q, *J* = 7.2 Hz, 4H), 3.80 (br, 1H), 3.35 (s, 2H), 1.26 (t, *J* = 7.2 Hz, 6H). To diethyl  $\alpha$ -benzyl  $\alpha$ -hydroxy malonate (6.3 g, 24 mmol) in 50 mL of EtOH (anhydrous) was added KOH (1.5 g). The mixture was stirred at rt over night. After removing the solvent in vacuo, the residue was taken up with 100 mL of ethyl acetate and 150 mL of water. The organic layer was removed. To the aqueous layer containing the potassium salt of the desired product was added 0.2 N HCl until pH = 2. The mixture was extracted with 200 mL ethyl acetate. The organic layer was dried with magnesium sulfate and concentrated to give the acid (2.6 g, 11 mmol, 46%) as a colorless oil. The racemic acid was then purified by chiral SFC (OJ-H, 4.6 × 100 mm, 5% MeOH/0.1% TFA/CO<sub>2</sub>, 2.5 mL/min, 100 bar) to give (2*R*)-2-benzyl-3-ethoxy-2-hydroxy-3-oxopropanoic acid as a single enantiomer (1.0 g, the first eluting peak). The assignment of the absolute configuration is based on vibrational circular dichroism (details in supporting information). LC/MS 261.1 (M+23). To a mixture of (2*R*)-2-benzyl-3-ethoxy-2-hydroxy-3-oxopropanoic acid (112 mg, 0.47 mmol), 3,5-dimethoxybenzylamine (86 mg, 0.51 mmol) and HATU (197 mg, 0.52 mmol) was added DMF (4 mL) and Hünig base (67 mg, 0.52 mmol). The mixture was stirred at rt for 2 h. To the mixture was added ethyl acetate and water. The organic layer was washed with water twice, and dried with magnesium sulfate. After removal of the solvent, the residue was purified by biotage (10–30% ethyl acetate in hexanes) to give ethyl (2*R*)-2-benzyl-3-[(3,5-dimethoxybenzyl)amino]-2-hydroxy-3-oxopropanoate (132 mg, 0.34 mmol, 72%) as a colorless oil. To a mixture of ethyl (2*R*)-2-benzyl-3-[(3,5-dimethoxybenzyl)amino]-2-hydroxy-3-oxopropanoate (40 mg, 0.10 mmol) and isocyanate **11** (80 mg, 0.54 mmol) in 4 mL of THF was added NaOH (solid, 50 mg) at rt. The mixture was under vigorous stirring for overnight. Filtered, and washed with ethyl acetate. The filtrate was concentrated, taken up by DMSO, and purified by Gilson (30–100% acetonitrile/water/0.05% TFA) to give **1g** (28 mg, 0.057 mmol, 57%) as a white solid. LC/MS 489.0 (M+1). <sup>1</sup>H NMR (300 MHz, CDCl<sub>3</sub>)  $\delta$ : 7.20–7.29 (m, 8H), 7.01 (d, *J* = 7.0 Hz, 2H), 6.80 (t, *J* = 5.5 Hz, 1H), 6.42 (t, *J* = 2.0 Hz, 1H), 6.35 (d, *J* = 2.0 Hz, 2H), 5.06 (q, *J* = 7.0 Hz, 1H), 4.44 (dd, *J* = 5.5, 14.5 Hz, 1H), 4.36 (dd, *J* = 5.5, 15.0 Hz, 1H), 3.79 (s, 6H), 3.65 (d, *J* = 14.0 Hz, 1H), 3.40 (d, *J* = 14.5 Hz, 1H), 1.54 (d, *J* = 7.0 Hz, 3H).